

IGR J16479-4514: the first eclipsing supergiant fast X-ray transient?

E. Bozzo^{1,2*}, L. Stella,¹ G. Israel,¹ M. Falanga,³ S. Campana,⁴

¹INAF - Osservatorio Astronomico di Roma, Via Frascati 33, 00044 Rome, Italy.

²Dipartimento di Fisica - Università di Roma Tor Vergata, via della Ricerca Scientifica 1, 00133 Rome, Italy.

³CEA Saclay, DSM/IRFU/Service d'Astrophysique (CNRS FRE 2591), F-91191, Gif sur Yvette, France.

⁴INAF - Osservatorio Astronomico di Brera, via Emilio Bianchi 46, I-23807 Merate (LC), Italy.

Received 2008 August 8; accepted 2008 September 19.

ABSTRACT

Supergiant fast X-ray transients are a new class of high mass X-ray binaries recently discovered with *INTEGRAL*. Hours long outbursts from these sources have been observed on numerous occasions at luminosities of $\sim 10^{36}$ – 10^{37} erg s^{−1}, whereas their low level activity at $\sim 10^{32}$ – 10^{34} erg s^{−1} has not been deeply investigated yet due to the paucity of long pointed observations with high sensitivity X-ray telescopes. Here we report on the first long (~ 32 ks) pointed *XMM-Newton* observation of IGR J16479-4514, a member of this new class. This observation was carried out in March 2008, shortly after an outburst from this source, with the main goal of investigating its low level emission and physical mechanisms that drive the source activity. Results from the timing, spectral and spatial analysis of the EPIC-PN *XMM-Newton* observation show that the X-ray source IGR J16479-4514 underwent an episode of sudden obscuration, possibly an X-ray eclipse by the supergiant companion. We also found evidence for a soft X-ray extended halo around the source that is most readily interpreted as due to scattering by dust along the line of sight to IGR J16479-4514. We discuss this result in the context of the gated accretion scenarios that have been proposed to interpret the behaviour of supergiant fast X-ray transient.

Key words: X-rays: binaries - binaries: eclipsing - stars: individual (IGR J16479-4514) - stars: neutron - X-rays: stars

1 INTRODUCTION

Supergiant Fast X-ray transients (SFXTs) are a new class of high mass X-ray binaries (HMXBs), recently discovered with *INTEGRAL*. These sources display sporadic outbursts lasting from minutes to hours with peak luminosities of $\sim 10^{36}$ – 10^{37} erg s^{−1}, and spend long time intervals at lower X-ray luminosities, ranging from $\sim 10^{33}$ erg s^{−1} to $\sim 10^{34}$ erg s^{−1}. In some SFXTs a very faint state, with a typical luminosity of $\sim 10^{32}$ erg s^{−1} has also been observed. The outbursts of SFXTs have so far been studied in relatively fairly detail, whereas the lower luminosity states remained poorly known due to the paucity of long pointings with high sensitivity X-ray telescopes. Data collected with both wide field instruments, such as *INTEGRAL*, and imaging X-ray telescopes, such as those on board *Chandra*, *Swift* and *XMM-Newton*, showed that the outburst spectra are well described by a power law of photon index $\Gamma \simeq 1$ –2 and an absorption column density that is larger than the interstellar Galactic value ($N_{\text{H}} \sim 10^{22}$ – 10^{23} cm^{−2}, Sguera et al. 2006; Walter et al. 2006). Similar spectral properties were inferred at luminosities of $\sim 10^{33}$ – 10^{34} erg s^{−1} (Walter et al. 2006; Sidoli et al. 2008), whereas indications were found that very

faint states might be characterized by significantly softer spectra (in't Zand 2005). The short duration of SFXT outbursts likely indicates the accretion flow towards the NS is not mediated by a disk (viscous timescales are of order of weeks to months). Instead, proposed models generally involve accretion onto a neutron star (NS) immersed in the clumpy wind of its supergiant companion (in't Zand 2005; Leyder et al. 2007; Walter & Zurita Heras 2007; Bozzo et al. 2008), and suggest these sources have orbital periods $\gtrsim 7$ –10 days (or, equivalently, orbital separations $\gtrsim 2.5 R_*$, with R_* the radius of the supergiant star).

Different models make different predictions with respect to properties and origin of states with luminosities below the outburst levels. Observations of these states, however, are still sparse and the properties of SFXTs at low luminosities are poorly known at present. It is generally believed that the X-ray luminosity in these states is powered by residual accretion onto the NS, taking place at much reduced rate than in outburst. In fact, large variations in the mass accretion rates in SFXTs are expected due to: i) a centrifugal and/or magnetic gating mechanism acting on a moderately clumpy wind (Bozzo et al. 2008); ii) clumps in the wind of the supergiant companion with extreme velocity and/or density contrasts (Walter & Zurita Heras 2007); iii) the presence of two components with different densities in the wind of the super-

* email: bozzo@oa-roma.inaf.it

giant companion (Sidoli et al. 2008). According to interpretation (i), the wide dynamic range in the X-ray luminosity (up to ~ 5 decades) displayed by SFXTs, if accompanied by a slow spin period ($\gg 100$ s), might indicate that these sources host “magnetars” (i.e., neutron stars with extremely high magnetic fields, $\sim 10^{15}$ G, Duncan & Thompson 1992). During very faint states, an important contribution to the X-ray luminosity may also derive from shocks in the strong wind of the OB supergiant star (in’t Zand 2005).

Here we report on the first long high sensitivity observation (~ 32 ks) of the SFXT IGR J16479-4514, when the source was in a low activity state. This source was detected in outbursts many times and appears to be characterized by a persistent luminosity of $\sim 10^{34}$ erg s $^{-1}$ (Sguera et al. 2008; Romano et al. 2008a; Walter & Zurita Heras 2007). The *XMM-Newton* target of opportunity observation was carried out after *Swift* discovered a very bright outburst from this source on March 19 (Romano et al. 2008b), and was aimed at investigating its low level emission and gaining insight in the physical mechanisms that drive its activity.

2 DATA ANALYSIS AND RESULTS

XMM-Newton (Jansen et al. 2001) observed IGR J16479-4514 between March 21 14:40:00UT and March 22 01:30:00UT for a total time span of ~ 37 ks. The EPIC-PN and EPIC-MOS cameras were operated in the small-window and full frame mode, respectively. We processed the observation data files (ODFs) by using the standard *XMM-Newton* Science Analysis System (SAS 7.1). The total effective exposure time was ~ 32 ks; the remaining observing time was discarded due to high radiation from solar activity. The EPIC-MOS data were strongly contaminated by single reflections photons from a nearby bright source (likely 4U 1642-45), and thus we report in the following on the analysis of the EPIC-PN data only. The extracted images, spectra and light curves were analyzed by using HEASOFT version 6.4. Figure 1 shows the 2-10 keV EPIC-PN light curve of the observation: in the first ~ 4 ks IGR J16479-4514 was caught during the decay from a higher (“A”) to a lower (“B”) flux state. The latter extended for most of the observation (~ 28 ks). We used a bin time of 1000 s in all the light curve fits; all errors are 90% confidence level. The mean count rate during state B was 0.024 ± 0.002 , i.e., a factor ~ 50 lower than the maximum count rate during state A. In order to search for spectral changes, we extracted light curves in the 2-5 keV and 5-10 keV bands. These are shown in the insert in Fig. 1 (first 8 ks of the observation). A fit with an exponential model plus a constant revealed a much slower decay in the soft band light curve: the e-folding time was 5400 ± 1500 s and 910 ± 100 s, in the 2-5 keV and 5-10 keV bands, respectively.

The energy spectra of states A and B are shown in Fig. 2, and were rebinned in order to have at least 20 counts per bin. Fits to these spectra were tried first by assuming an absorbed power law plus a Gaussian line at ~ 6.4 keV. This model provided a good fit to the spectrum of state A (reduced $\chi^2=1.1$) for a flatter power law index ($0.4_{-0.4}^{+0.5}$) than previously measured for the source (1.6 ± 0.2 , Sidoli et al. 2008)). The absorption column density was marginally larger ($1.2_{-0.3}^{+0.6} \times 10^{23}$ cm $^{-2}$ as opposed to $\sim 7 \times 10^{22}$ cm $^{-2}$). During state B this simple model gave a poorer fit (reduced $\chi^2=1.7$), a much reduced column density ($4.0_{-0.7}^{+0.6} \times 10^{22}$ cm $^{-2}$) and a power law index compatible with that of state A. The equivalent width (EW) of the Fe fluorescence line at ~ 6.4 keV showed a striking increase from ~ 260 eV (state A) to ~ 900 eV (state B). This indicated that in state B (most of) the X-ray flux from the source was obscured along our line of sight, but kept on shining on the Fe-

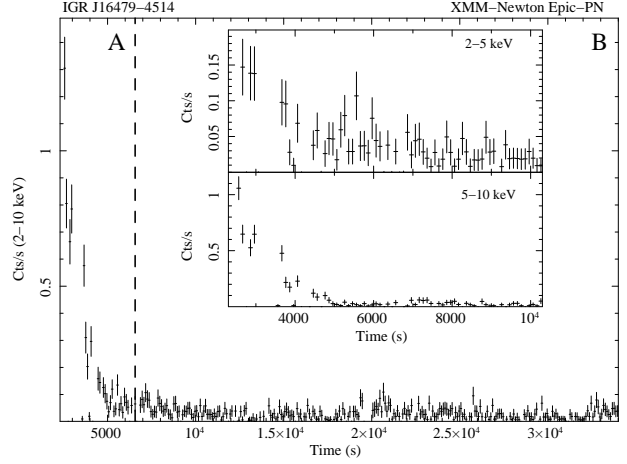


Figure 1. EPIC-PN light curve of IGR J16479-4514 in the 2-10 keV band. The bin time is 100 s and the start time is March 21 16:42:42UT. During the first 4 ks of the observation the source flux decayed from a higher (“A”) to a lower (“B”) level. The insert in the figure shows the first 8 ks of the observation in the 2-5 keV and 5-10 keV energy bands.

line emitting material. The shape of the light curve (see Fig. 1) and evolution of the spectrum across the state A-state B transition presented also remarkable similarities with the eclipse ingress of eclipsing X-ray sources such as OAO 1657-415 (Audley et al. 2006). Moreover the slower decay of the soft X-ray light curve (in turn similar to that observed in OAO 1657-415) suggested that IGR J16479-4514 is seen through an extended dust-scattering halo (see e.g., Day & Tennant 1991; Nagase et al. 1992).

To confirm this we analysed the radial distribution of the X-ray photons detected from IGR J16479-4514 and compared it with the point spread function (PSF) of the *XMM-Newton* telescope/EPIC-PN camera (HEW of $\sim 12.5''$). We did this separately in the 2-5 keV and 5-10 keV bands for states A and B. The results are shown in Fig. 4. The radial distribution of photons from IGR J16479-4514 was compatible with the *XMM-Newton* PSF for both energy ranges during state A and for the 5-10 keV range during state B. On the contrary the 2-5 keV source photons during state B had a considerably more extended distribution than the *XMM-Newton* PSF. This behaviour is precisely the one expected from a quickly obscured source seen through a dust scattering halo: soft X-ray photon emitted when the source is unobscured are scattered along our line of sight by interstellar dust, reaching us also after X-ray source obscuration, as a results of the longer path that they follow. The dust scattering halo is most prominent at low energies (due to the energy dependence of the scattering cross section) and when the source is obscured, because contamination by direct photons from the source is virtually absent. For a halo size θ of tens of arcsec radius (see the top-right panel of Fig. 3) and the estimated source distance of 4.9 kpc (Rahoui et al. 2008), the longer path followed by scattered photons gives rise to a delay (see e.g., Thompson & Rothschild 2008)

$$\delta t = 5.3 d_{4.9\text{kpc}} (\theta/\text{arcsec})^2 x/(1-x) \sim 5300 \text{ s}, \quad (1)$$

where x is the fractional distance of the halo from the source, $d_{4.9\text{kpc}}$ is the source distance in unit of 4.9 kpc, and we used $\theta=30''$ and $x=1/2$. The typical delay is thus of few hours, in agreement with the e-folding decay time of the soft X-ray light curve in state B.

Motivated by the above findings we considered the spectral

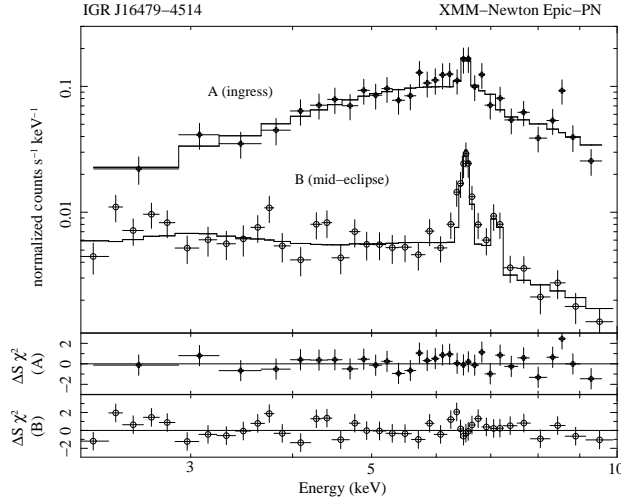


Figure 2. 2-10 keV spectra extracted from intervals A and B of Fig. 1. The best fit models and the residuals from these fits are also shown (see Sect. 2).

model that has been used in studies of eclipsing X-ray binaries seen through a dust-scattering halo, that is (Audley et al. 2006; Ebisawa et al. 1996)

$$I(E) = e^{\sigma(E)N_H} [I_s E^{-\alpha} + e^{\sigma(E)N_{Hw}} I_w E^{-\alpha} + e^{\sigma(E)N_{Hd}} I_d E^{-\beta} + I_{ln1} e^{-(E-E_{ln1})^2/(2\sigma_{ln1}^2)} + I_{ln2} e^{-(E-E_{ln2})^2/(2\sigma_{ln2}^2)}] \quad (2)$$

Here the continuum consists of three components seen through an interstellar column density of N_H : two power laws with “the same” photon index α (normalizations I_s and I_w), and a third power law with photon index $\beta=\alpha+2$ (normalization I_d). The two power laws with the same photon index represent respectively, the source emission that is received directly at the earth (i.e., the direct component), and the source emission that is scattered along our line of sight by material in the immediate surroundings of the X-ray source, likely the wind from the massive companion star (we term this “wind scattered component”). The scattered component will preserve the slope of the incident spectrum, while photoelectric absorption by the wind material can in principle reduce the number of low energy photons that are scattered, thus mimicking a higher column density in the scattered component. This is why the wind scattering term in Eq. 2 comprises an extra absorption component (N_{Hw}). Iron features (around ~ 6.4 keV and ~ 7.0 keV see Fig. 2) are represented by the Gaussians in Eq. 2 and arise also from reprocessing of the source radiation in the wind. The direct component is expected to dominate the X-ray emission when the source is out of eclipse. As the NS approaches the companion’s limb, the source photons directly reaching us will propagate through denser and denser regions of the companion’s wind, such that increased photoelectric absorption is to be expected shortly before the eclipse ingress ($N_{Hd} \gtrsim N_{Hw}$). The third power law component, with photon index $\beta=\alpha+2$, originates from small angle scattering of (mainly) direct photons off interstellar dust grains along the line of sight (Day & Tennant 1991; Nagase et al. 1992); therefore, it should be characterized by a similar column density to that of the direct component away from eclipse. The dust scattering cross section decreases steeply for increasing photon energies, such that the spectrum of the scattered photons is softened by a factor of E^{-2} . Both the wind and dust scattered components are expected to be most

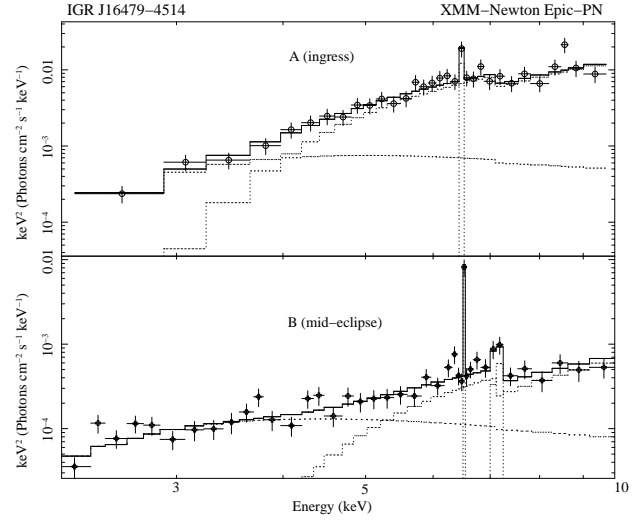


Figure 3. 2-10 keV unfolded spectra of Fig. 2. The best fit model components are displayed with dotted lines.

prominent during the eclipse, when the direct component is occulted by the companion star.

Owing to limited statistics and degeneracy in some of the spectral fit parameters, it proved impossible to disentangle the contribution from the two power laws of index α in the *XMM-Newton* spectra of IGR J16479-4514. In practice we fitted a model with only two continuum components, a single power law of slope α (with normalisation I_α and column density $N_{H,\alpha}$) and a power law of slope β (with normalisation I_β and column density $N_{H,\beta}$). The former component was taken to approximate the sum of the two α -slope power laws in Eq. 2, with the direct component dominating before the eclipse ingress and the wind scattered component dominating during the eclipse. The relevant model was thus

$$I(E) = e^{\sigma(E)N_{H,\beta}} I_\beta E^{-\beta} + e^{\sigma(E)N_{H,\alpha}} [I_\alpha E^{-\alpha} + I_{ln1} e^{-(E-E_{ln1})^2/(2\sigma_{ln1}^2)} + I_{ln2} e^{-(E-E_{ln2})^2/(2\sigma_{ln2}^2)}]. \quad (3)$$

We kept α fixed at 0.98, the best fit value found by Romano et al. (2008a) when the source was in outburst (and thus away from an X-ray eclipse); consequently we fixed also $\beta=2.98$. The best fit models are shown in Fig. 2, and the corresponding parameters are given in Table 1. In Fig. 3 we plot also the unfolded spectra. While in state A, a power law component with slope α plus a Gaussian line at ~ 6.5 keV (EW of ~ 190 eV) provided a reasonably good fit also for a fixed value of $\alpha \sim 0.98$ ($\chi^2/\text{d.o.f.}=33/28$). However, adding the dust scattered component significantly improved the fit ($\chi^2/\text{d.o.f.}=20.4/26$). In state A the relatively high source flux and small EW of the iron fluorescence line testifies that (most of) the emission is likely due to the direct component. In order to investigate this, we also accumulated spectra during the first 1.5 ks and last 2.5 ks of state A (not shown in Fig. 2). These two spectra were reasonably fit ($\chi^2/\text{d.o.f.}=18.6/16, 13.3/9$) by assuming an absorbed powerlaw with fixed photon index 0.98 and an absorption column density of $30^{+8}_{-7} \times 10^{22} \text{ cm}^{-2}$ and $5.6^{+3.8}_{-3.0} \times 10^{22} \text{ cm}^{-2}$, respectively (the addition of a Gaussian line at ~ 6.5 keV did not significantly improve any of these fits). We interpreted the decreasing absorption column density revealed by these fits as the effect of a change in the dominating spectral component during the early ingress to the eclipse. Specifically, the direct component dominates the first

part of the state A and is absorbed by the very dense companion's limb; instead, most of the X-ray emission during the last 2.5 ks of this state is likely due to the wind scattered component, which is in turn absorbed by a lower dense material, in agreement with the expectation $N_{\text{Hd}} \gtrsim N_{\text{Hw}}$ discussed above.

In state B, the ratio I_α/I_β is larger than the corresponding value obtained during state A, indicating a dust scattering halo whose intensity decreases slowly during the eclipse. The intensity of the power law of slope α decreased substantially, while the EW of the Fe-line at ~ 6.5 keV increased to ~ 770 eV. We also found evidence ($\sim 2\sigma$) for an additional Fe-line at ~ 7.1 keV with a ~ 300 eV EW, consistent with being the K_β . Owing to the poor statistics of the present observation, we were unable to investigate further the nature of this line; however, we note that the ratio between the normalizations of the K_α and K_β lines, as inferred from fits in Table 1, is roughly in agreement with the expected value ~ 0.15 – 0.16 (see e.g., Molendi et al. 2003; Ibarra et al. 2007). The most natural interpretation of this is that in state B the direct emission component is occulted along our line of sight, while the spectrum we observe is the sum of a dust scattered component, dominating at lower energies, and a wind scattered component characterised by a high absorption. The marked increase in the EW of the Fe-line at ~ 6.5 across the state A-state B transition testifies that the region where the line is emitted is larger than the occulting body (the superegiant companion, if we are dealing with an eclipse); this provides strong evidence that the uneclipsed emission in state B at hard X-ray energies (the α -slope power law) arises mostly from photons scattered by the wind in the immediate surrounding of the source. In both states A and B the measured $N_{\text{H},\beta}$ is consistent with the absorption column density reported by Romano et al. (2008a); this provides further support in favour of the β -slope power law representing the outburst emission seen through a dust scattering halo with a delay of $\gtrsim 1$ hour. These findings and interpretation are in line with those that emerged from detailed studies of some per-se eclipsing HMXBs.

We obtained also spectral fit in which α was allowed to vary as free parameters, while $\beta = \alpha + 2$. However, this did not lead to a significant improvement of any of the fits, while the best fit parameters were consistent with the ones found above.

No evidence for a coherent modulation was found in the present data up to periods of ~ 1000 s (3σ upper limit in the 80%–90% pulse fraction¹ range).

3 DISCUSSION AND CONCLUSION

We reported on the first long (~ 32 ks) pointed observation of IGR J16479-4514 during a period of low X-ray emission. The decay of the light curve and the increase of the iron line EW between states A and B, likely indicated that the X-ray radiation from this source was being obscured by an occulting body. Based on the present knowledge of IGR J16479-4514, we suggested that *XMM-Newton* might have caught the source entering an X-ray eclipse. The possibility that the obscuration event was caused by a wind clump cannot be excluded at present. However, we regard this interpretation as unlikely, because photoelectric absorption would be expected to cause a more pronounced flux decrease at soft X-ray energies than at hard X-ray energies (at least in the early stages of

Table 1. Best fit parameters of the spectra during states A and B. $F_{2-10 \text{ keV}}$ is the absorbed flux in the 2–10 keV band, and the X-ray luminosity L_X is derived from this flux assuming a source distance of 4.9 kpc (Rahoui et al. 2008). Errors are at 90% confidence level.

FIT PARAMETERS	STATE “A”	STATE “B”
$N_{\text{H},\alpha}$ (10^{22} cm^{-2})	35^{18}_{-13}	54^{26}_{-25}
$N_{\text{H},\beta}$ (10^{22} cm^{-2})	9^{+9}_{-6}	6^{+1}_{-2}
I_α	$1.8^{0.4}_{-0.3} \times 10^{-3}$	$1.1^{0.5}_{-0.4} \times 10^{-4}$
α	0.98 (frozen)	0.98 (frozen)
I_β	$5^{+8}_{-4} \times 10^{-3}$	$8^{+2}_{-3} \times 10^{-4}$
β	2.98 (frozen)	2.98 (frozen)
E_{ln1} (keV)	$6.53^{0.06}_{-0.07}$	$6.51^{0.03}_{-0.02}$
I_{ln1}	$5^{+3}_{-3} \times 10^{-5}$	$1.8^{1.0}_{-0.4} \times 10^{-5}$
EW_{ln1} (keV)	0.15	0.77
E_{ln2}	-	$7.11^{0.06}_{-0.09}$
I_{ln2}	-	$8^{+7}_{-4} \times 10^{-6}$
EW_{ln2} (keV)	-	0.28
$\chi^2/(\text{d.o.f.})$	20.4/26	36.5/33
$F_{2-10 \text{ keV}}$ ($10^{-13} \text{ erg cm}^{-2} \text{ s}^{-1}$)	1.0×10^2	7.5
L_X ($10^{33} \text{ erg s}^{-1}$)	29.0	2.2

the obscuration event) contrary to the results presented here. On the other hand, an energy-independent obscuration could be caused by a fully ionized clump that is optically thick to electron scattering, a very unlikely possibility in consideration of the low X-ray luminosity of the source. Obscuration by a tilted accretion disk, which is known to cause similar effects in other HMXBs (see e.g., Zane et al. 2004), also does not appear as a very promising possibility here. This is because the outbursts of IGR J16479-4514, and SFXT in general, have durations that are incompatible with viscous timescales in a typical accretion disc (see Sect. 1).

In order to interpret the source flux and spectral variations revealed by the *XMM-Newton* observation, we considered the same scenario that has been extensively discussed for eclipsing HMXBs with a dust scattering halo (see e.g., Audley et al. 2006; Ebisawa et al. 1996): during the eclipse ingress source photons reaching us directly dominated the X-ray flux we observed; while in eclipse the residual X-ray flux is due to the sum of a wind-scattered component and a dust scattering halo. Strong evidence for the wind scattered component in the case of IGR J16479-4514 comes from the marked increase of the EW of the iron fluorescence line at ~ 6.5 keV. A tens of arcsec wide dust-scattering halo around IGR J16479-4514 could be directly seen in the soft X-ray *XMM-Newton* images accumulated during the eclipse. Moreover the residual soft X-ray decreased on a timescale of ~ 1 hr after the eclipse onset, as expected for a dust scattering halo of the size seen by *XMM-Newton* at the source distance of 4.9 kpc.

We conclude that IGR J16479-4514 is the first SFXT that displayed evidence for an X-ray eclipse. In this case, some constraints on the orbital period of this system can be derived by using (Rappaport & Joss 1983)

$$R_* = a [\cos^2 i + \sin^2 i \sin \Theta_e]^{1/2}. \quad (4)$$

Here i is the inclination of the orbit to the plane of the sky, Θ_e is the

¹ Here for pulse fraction we mean the ratio between the pulsed emission and the total emission from the NS.

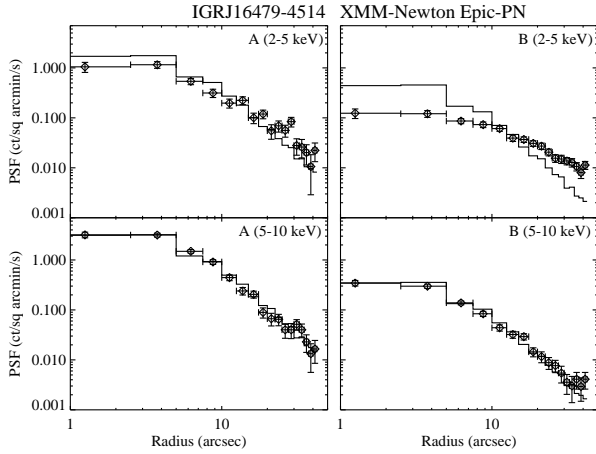


Figure 4. *XMM-Newton* EPIC-PN PSF as a function of the distance from the source. The upper panels are for images extracted in states A and B in the energy range 2-5 keV. Instead, the PSF in the lower panels are extracted from the same images but in the 5-10 keV energy range. For this analysis we used the XIMAGE tool (version 4.4).

eclipse half-angle, a is the binary separation, and we assume in the following a supergiant star with a mass of $\sim 30 M_{\odot}$ and a radius of $R_{*} \sim 20 R_{\odot}$. We consider circular orbits, as it is generally expected for an HMXB with a supergiant companion (Rappaport & Joss 1983). By using Kepler's law, Eq. 4 can be solved for the orbital period, as a function of the inclination angle, for any fixed value of the eclipse duration. This is shown in Fig. 5. The solid line in this figure represents the solution obtained by assuming an eclipse duration of ~ 28 ks. This value should be regarded as a lower limit on Θ_e , since in the *XMM-Newton* observation discussed here there is no evidence for the eclipse egress. The dashed line is for an eclipse that lasts for 55 ks (chosen for comparison with the previous case), whereas the triple-dot-dashed line is for an eclipse that extends for half of the binary orbital period. The latter provides an upper limit on Θ_e . We also include in the figure, the lower limit on the orbital period that was obtained by Negueruela et al. (2008), by assuming the sporadic outbursting activity of SFXTs is related to accretion of clumps from the supergiant stellar wind (see Sect. 1). If we consider that the clumpy wind model applies to IGR J16479-4514, then the region of allowed parameter space in Fig. 5 suggest this source is a high inclination SFXT. From this figure we also note that, for this source, an eclipse with a duration much longer than the ~ 28 ks observed here is very unlikely: in fact the longer is the duration of the eclipse, the smaller is the allowed parameter region in Fig. 5. In particular, a much longer eclipse would require a very high inclination angle and short orbital period that can be hardly reconciled with the requirements of the clumpy wind model (the NS orbit should be very close to the supergiant surface, and a persistent luminosity of $\gtrsim 10^{36}$ erg s $^{-1}$ would be expected).

Walter & Zurita Heras (2007) derived the average quiescent flux of IGR J16479-4514 as observed by *INTEGRAL* over ~ 67 d, which converts to an X-ray luminosity of few 10^{34} erg s $^{-1}$. This relatively high luminosity is comparable with that of state A, and thus provides support in favor of state B being an unfrequent state, as expected in the eclipse interpretation (eclipses cannot last more than half of the orbital period).

At present, it is not clear whether eclipses should be expected also in other SFXTs. However, we note that, if other SFXTs display X-ray eclipses, their maximum luminosity swing might not be due

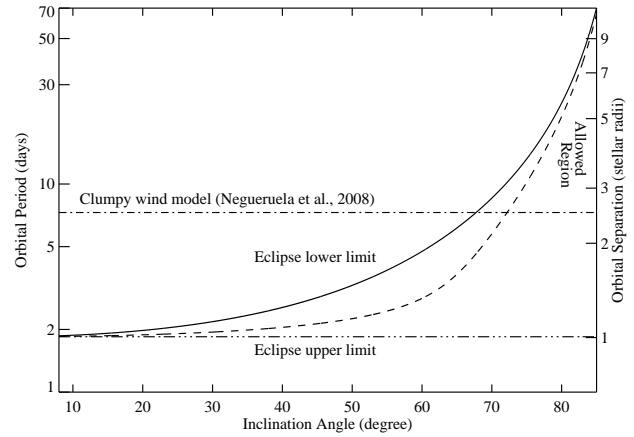


Figure 5. Orbital period constraints on IGR J16479-4514, as a function of the binary inclination angle. The solid line is given by Eq. 4 assuming an eclipse duration of 28 ks, the dashed line is for an eclipse duration of 55 ks, and the triple-dot-dashed line is for an eclipse lasting half of the binary orbital period. The dot-dashed line is the lower limit on the orbital period obtained by applying the clumpy wind model to IGR J16479-4514. According to this model, the region of allowed parameters in this plot indicates IGR J16479-4514 is a high-inclination SFXT.

to genuine changes in the mass accretion rate, impacting on the application of the gating accretion model for SFXT (Bozzo et al. 2008). Further observations of IGR J16479-4514, as well as other SFXTs in quiescence, will improve our knowledge of the low level emission of these sources, and will help clarifying this issue.

ACKNOWLEDGMENTS

We thank Norbert Schartel and the *XMM-Newton* staff, for executing this ToO observation, and the referee Roland Walter for useful comments and suggestions. EB thanks E. Piconcelli for useful discussions. This work was partially supported through ASI and MIUR grants.

REFERENCES

- Audley, M.D., Nagase, F., Mitsuda, K., Angelini, L., Kelley, R.L. 2006, *MNRAS*, 367, 1147
- Bozzo, E., Falanga M., Stella L. 2008, *ApJ*, 683, 1031
- Day, C.S.R. & Tennant, A.F. 1991, *MNRAS*, 251, 76
- Duncan, R. C. & Thompson, C. 1992, *ApJ*, 392, L9
- Ebisawa, K., Day, C.S.R., Kallman, T.R., Nagase, F., Kotani, T., Kawashima, K., Kitamoto, S., Woo, J.W. 1996, *PASJ*, 48, 425
- Ibarra, A., Matt, G., Guainazzi, M., Kuulkers, E., Jimnez-Bailin, E., Rodriguez, J., Nicastro, F., Walter, R. 2007, *A&A*, 465, 501
- in 't Zand 2005, *A&A*, 441, L1
- Jansen, A., Lumb, D., Altieri B., et al. 2001, *A&A*, 365, L1
- Leyder, J.-C., Walter, R., Lazos, M., Masetti, N., & Produit, N. 2007, *A&A*, 465, L35
- Molendi, S., Bianchi, S., Matt, G. 2003, *MNRAS*, 343, L1
- Nagase, F. 1989, *PASJ*, 41, 1
- Nagase, F., Corbet, R.H.D., Day, C.S.R., Inoue, H., Takeshima, T., Yoshida, K., Mihara, T. 1992, *ApJ*, 396, 147

- Negueruela, I., Torrejon, J. M., Reig, P., Ribo, M., & Smith, D. M. 2008, preprint (astro-ph/0801.3863)
- Rahoui, F., Chaty, S., Lagage, P., Pantin, E. 2008, preprint (astro-ph/0802.1770)
- Rappaport, S.A. & Joss, P.C. 1983, in *Accretion-driven stellar X-ray sources*, 1
- Romano, P., et al. 2008a, *ApJ*, 680, L137
- Romano, P., et al. 2008b, *Astr. Tel.*, 1435
- Sguera, V., et al. 2006, *ApJ*, 646, 452
- Sguera, V., et al. 2008, preprint (astro-ph/0805.0496)
- Sidoli, L., et al. 2008, preprint (astro-ph/0805.1808)
- Thompson, T.W.J. & Rothschild, R.E. 2008, preprint (astro-ph/0806.2859)
- Walter, R., et al. 2006, *A&A*, 453, 133
- Walter, R. & Zurita Heras, J. A. 2007, *A&A*, 476, 335
- Zane, S., Ramsay, G., Jimenez-Garate, M.A., Willem den Herder, J., Hailey, C.J. 2004, *MNRAS*, 350, 506